A Model for Self-Assembly in Side Chain Liquid Crystalline Block Copolymers

Manas Shah, Victor Pryamitsyn, and Venkat Ganesan*

Department of Chemical Engineering, University of Texas at Austin, Austin, Texas 78712

Received July 13, 2007; Revised Manuscript Received October 23, 2007

ABSTRACT: We present a new model based on self-consistent field theory (SCFT) approach and complement it by strong segregation theory (SST) based calculations to characterize the self-assembly behavior in side-chain liquid crystalline block copolymers. Our model considers a micromechanical representation of flexible coil−coil diblock copolymers, with rodlike units grafted to one of the blocks. We present results which elucidate self-assembly arising from the interplay between block copolymer microphase separation and the orientational ordering of the rod segments. We determine the morphological phase diagram for this system by assuming two dimensional variations of composition profiles. Our numerical results are in very good agreement with reported experimental observations. Many of the traditional flexible diblock copolymer microphases are also predicted to occur for side chain liquid crystalline polymers, with smectic ordering accompanying within the microphases. The equilibrium phase morphologies are observed to depend on the molecular weight of the copolymer, the length of the rod units, the relative volume fractions of each block, and the energetic and orientational interactions between different components. Moreover, for the parameters considered in this article, microphase separation was observed to be a requisite for developing orientational ordering between mesogenic units. The results of SST provide a physical explanation for the observations and are in good agreement with that of the SCFT calculations.

I. Introduction

The self-assembly behavior of *flexible* diblock and multiblock copolymers have been extensively studied from both theoretical and experimental viewpoints. Their morphological characteristics are known to be parametrized by the fraction of the different blocks and by the incompatibility between the different blocks. Some of the commonly observed self-assembled microstructures in such polymers include lamellar phases, hexagonally packed cylinders, body centered cubic spheres, and bicontinuous gyroid phases.[1] In contrast, liquid crystalline polymers (LCP) are a special class of polymers possessing mesogenic units capable of orientational ordering in addition to morphological assembly. Such polymers have attracted significant attention in view of their potential applications in electrooptical display devices and high strength fibers.[2] The self-assembly characteristics of block copolymers containing such LC units are expected to be richer than flexible diblock copolymers due to the combined possibility of microphase separation along with orientational ordering of the segments. For instance, rod−coil diblock copolymers have displayed morphological characteristics distinct from that of conventional flexible block copolymer mesophases which includes phases such as arrowhead, zigzag, wavy lamellar, and smectic bilayers.[3−5]

Side-chain liquid crystalline (SCLC) block copolymers are a special class of liquid crystalline polymers consisting of side-chain mesogenic units attached typically through an alkyl spacer to an amorphous backbone. Several experimental groups have synthesized and studied the properties of side chain liquid crystalline block copolymers.[7−10] In contrast to the morphologies exhibited by rod−coil block copolymers, side-chain liquid crystalline block copolymers exhibit richer self-assembly characteristics that manifest an interplay between the backbone block copolymer ordering and liquid crystalline ordering between side chain rod units.[11] Overall, at low volume fractions of the amorphous coil block (i.e., the ungrafted flexible block), hexagonally closed packed cylinders of the coil phase have been observed inside a continuous matrix made of the LC block.[9,10,12−14] The rod segments were observed to be oriented parallel to the block copolymer interface and along the axis of the cylinders.[13,14] Increasing the volume fraction of the amorphous coil block have been shown to lead initially to perforated lamellar morphologies (possibly metastable states), in which alternating lamellar phases are interspersed with cylindrical domains in which the coil block is confined.[12] In most experiments, further increase in the volume fraction of the coil block leads to a broad lamellar regime which persists up to relatively low volume fractions of the block on which the mesogens are grafted (hereafter referred to as LC block). Moreover, it has been observed that the lamellar domains typically stabilize the formation of Smectic C* phases where the orientation of the rod segments are parallel to the block copolymer interface.[7,15] However, in some cases, especially when the rods are connected through a longer alkyl spacer to the main chain backbone, rod orientations perpendicular to the block copolymer interface have also been observed.[15] At high volume fractions of the amorphous coil block, cylindrical microdomains of LC blocks, with the mesogens parallel to the axis of cylinders have been observed.[9] Moreover in most of the experiments reported, orientational ordering of the rod segments occurs at or after the order−disorder transition (ODT) for the microphase separation, suggesting that the onset of compositional ordering significantly influences the orientational ordering of the rods.

In contrast to the significant theoretical developments accompanying self-assembly in flexible block copolymers, methods and models for predicting the self-assembly behavior of side chain liquid crystalline block copolymers are very limited. A scaling-based free energy model was developed for the side chain liquid crystalline block copolymers by Anthamatten and co-workers.[16] This model accounts for the orientational interaction of mesogens, stretching of the amorphous chains, surface tension of the interfaces between the incompatible blocks and the elastic deformation of the LC phase.[16] Free energies were estimated for different morphologies and phase diagrams were

10.1021/ma071566b CCC: $40.75
Published on Web 12/07/2007

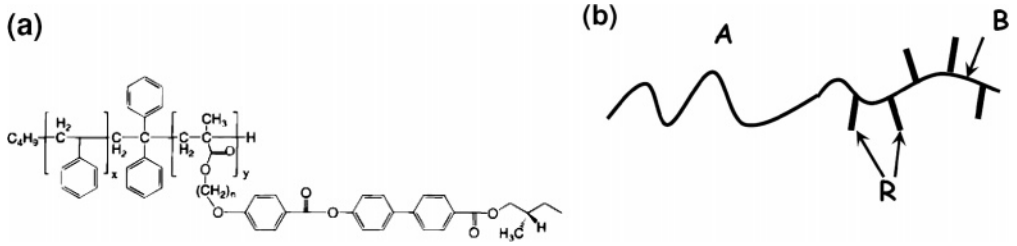

Figure 1. (a) Molecular structure of a SCLC copolymer used in the experiments of Hammond and co-workers.[15] (b) Schematic of our model for side chain liquid crystalline polymer. N_A monomers of A block is attached with a B block having N_R number of attached mesogenic units.

constructed which were reported to be in qualitative agreement with the experiments. On a slightly different front, some theoretical models based on self-consistent field theory (SCFT) and random phase approximation (RPA) have considered the self-assembly characteristics of comb−coil block copolymers (which can be argued to be architecturally similar to side chain liquid crystalline block copolymers).[17−19] The SCFT model considered the general case of combs grafted at arbitrary locations along the backbone. Because of computational limitations, such a model could only study the self-assembly behavior of the polymer with a few number of grafted units.[17] The RPA formalism on the other hand is limited to weak segregation regime, and requires one to consider known structures whose free energies are then compared.[19] Consequently, it is somewhat limited to "discover" structures in complex polymers such as SCLC multiblock copolymers.

In this article, we propose a combined study based on self-consistent mean field theory (SCFT) and strong segregation theory (SST) to understand the self-assembly characteristics of side chain liquid crystalline (SCLC) block copolymers. SST is analytical in nature and therefore identifies the physics behind the self-assembly characteristics. SST has been shown to be very successful in describing the phase behavior of diblock and multiblock copolymers accurately at stronger segregations.[1,20,21] For SCLC polymers, the strong segregation approximation we use is expected to be more accurate for relatively shorter rod molecules grafted to the main chain backbone. In contrast, the self-consistent mean field theory is numerical, but in principle is valid for all degrees of segregation and rod lengths. We view these methods as complementary, and use them together to provide a complete overview of the self-assembly behavior.

Figure 1a displays the molecular structure of a SCLC block copolymer used in the experiments of Hammond and co-workers, in which a styrene block is linked to a methacrylate block on which mesogenic chiral biphenyl benzoate molecules are grafted through an alkyl spacer.[15] Inspired by the structure of such molecules, we develop a SCFT model based on the micromechanical representation of the SCLC block copolymer as having a coil block (A) linked to another coil block (B). The monomers of the coil block (B) are assumed to be linked to each other through flexible spring like units. Each monomer of the B coil is also assumed to be attached to a mesogenic unit (R) (shown schematically in Figure 1b). As we demonstrate later, this approach eliminates the constraint of incorporating only a "few" grafted side chains (which typically increases the computational requirements), and instead models the experimental conditions more realistically. The SST model adopts a more simplistic view by ascribing the effect of rods to two contributions: (i) An increased monomeric volume of the B segments; (ii) The influence of changes in orientational entropies and interaction energies due to ordering of the rods within mesophases. These contributions are then combined with the classical theory of ordering in flexible diblock copolymers to discern the self-assembly characteristics in the system.

The rest of the article is organized as follows. In section II, we demonstrate the manner in which the thermodynamical features of the above model can be recast into a field theory model which can be treated by mean-field approximation to lead to a self-consistent field theory for SCLC block copolymer. In section III, we present results for the self-assembly characteristics by assuming two-dimensional morphologies. Our results relate the morphological characteristics of SCLC block copolymers to various parameters such as its overall molecular weight, the length of the rod units, the volume fraction of each block and the orientational interaction between LC moieties. We explore a limited subset of the parametric space, and we present results which are in good agreement with experimental results. These results suggest that our model provides a means to deduce the morphologies and orientational characteristics for other parametric conditions of SCLC block copolymer. In section IV, we present a description of the model for SST calculations, the accompanying results, and a comparison to the corresponding SCFT results.

II. Description of SCFT Model and Framework

In this section, we present a field theoretic formulation of the model for the side chain liquid crystalline diblock copolymer described in the introduction (Figure 1b). The theoretical framework parallels the earlier developments in models for flexible diblock copolymers and rod−coil copolymers,[1,3] however differing in the presence of side chain rod units at every monomer of one of the blocks.

We consider a canonical ensemble of an incompressible melt of n side chain liquid crystalline block copolymers in a volume V. Each polymer is assumed to be made of a block of a flexible chain (referred to as the A block) attached to another flexible block (B) to which the rodlike units (R) are attached. Closely modeling the experiments of SCLC polymers, we assume that side chain mesogenic units are attached to every monomer of the B block. Between two rod units, the backbone of the B polymer is modeled as a flexible Hookean spring. The monomeric units of the flexible coil (A and B) are both assumed to be characterized by the same statistical segment length b. For simplicity, we assume that both coil and rod monomers occupy the same volume (ρ_0^{-1}). On the basis of this assumption, we define the characteristic length of a rod monomer "a", such that $ad^2 = \rho_0^{-1}$ (d being the diameter of the rod). The rod unit is then assumed to contain "m" such monomers. This parametrization is identical to that employed in earlier models of rod−coil block copolymers.[3,23] In this notation, if there are N_A monomers of A and N_R number of rod units (equal to number of B monomers), then the overall number of units of the SCLC polymer is

$$N = N_A + N_R(m + 1) \tag{1}$$

The volume fraction of the amorphous block is denoted as f_A ($= N_A/N$), and the volume fractions of the B and R monomers are denoted as f_B ($= N_R/N$) and f_R ($= mN_R/N$) respectively.

The flexible (A and B) parts of the copolymer are parametrized with a continuous variable "s" which monotonically increases along the length of the polymer. Explicitly, $s = 0$ at the beginning of A-block, $s = N_A$ at the junction of the two blocks, and $s = N_A + N_R$ at the end of B block. Using this parametrization, the function $\mathbf{R}_\alpha(s)$ (where $\alpha = 1, 2, ..., n$ indexes the different polymers) is used to describe the conformations of the flexible A block and backbone monomers. Each rod block whose ends are at $\mathbf{R}_\alpha(s)$ ($N_A < s \leq N_A + N_R$), are assumed to be oriented along a unit orientational vector denoted as $\mathbf{u}_\alpha(s)$. On the basis of these notations, the nondimensional volume fractions for A, B, and R segments are denoted $\hat{\phi}_A(\mathbf{r})$, $\hat{\phi}_B(\mathbf{r})$, and $\hat{\phi}_R(\mathbf{r})$, and are defined as

$$\hat{\phi}_A(\mathbf{r}) = \frac{1}{\rho_0}\sum_{\alpha=1}^{n}\int_0^{N_A} ds\, \delta(\mathbf{r} - \mathbf{R}_\alpha(s))$$

$$\hat{\phi}_B(\mathbf{r}) = \frac{1}{\rho_0}\sum_{\alpha=1}^{n}\int_{N_A}^{N_A+N_R} ds\, \delta(\mathbf{r} - \mathbf{R}_\alpha(s))$$

$$\hat{\phi}_R(\mathbf{r}) = \frac{1}{\rho_0}\sum_{\alpha=1}^{n}\int_{N_A}^{N_A+N_R} ds \int_0^m dp\, \delta(\mathbf{r} - \mathbf{R}_\alpha(s) - ap\mathbf{u}_\alpha) \quad (2)$$

In addition, to describe the orientational interactions between the rods, we invoke an orientational order parameter $\hat{\mathbf{S}}(\mathbf{r})$ defined as

$$\hat{\mathbf{S}}(\mathbf{r}) = \frac{1}{\rho_0}\sum_{\alpha=1}^{n}\int_{N_A}^{N_A+N_R} ds \int_0^m dp\, \delta(\mathbf{r} - \mathbf{R}_\alpha(s) - ap\mathbf{u}_\alpha)\left[\mathbf{u}_\alpha\mathbf{u}_\alpha - \frac{\mathbf{I}}{3}\right] \quad (3)$$

The overall melt is assumed to be incompressible i.e.,

$$\hat{\phi}_A(\mathbf{r}) + \hat{\phi}_B(\mathbf{r}) + \hat{\phi}_R(\mathbf{r}) = 1 \quad (4)$$

Energetic interactions in the above model are assumed to be comprised of the following components. (i) Stretching free energy of the flexible chain ($H_0(\mathbf{R})$): Within the Gaussian chain model, this is given as[3,25]

$$H_0[\mathbf{R}] = \frac{3}{2b^2}\sum_{\alpha=1}^{n}\int_0^{N_A+N_R} ds \left|\frac{d\mathbf{R}_\alpha(s)}{ds}\right|^2 \quad (5)$$

(ii) The enthalpic energy associated with the unfavorable interactions between the different blocks: We quantify these interactions in terms of two Flory−Huggins interaction parameters, χ_{ABR} representing the interaction between A block and the combined units of B and R blocks, and χ_{BR} representing the interaction between B and R units. In principle, a more general representation will involve three parameters describing the interactions between A and B, B and R, and A and R units. However, we adopt the proposed representation to simplify the parameter space. In terms of these interaction parameters, the enthalpic contributions to the free energy can be expressed as

$$H_1[\mathbf{R}] = \chi_{ABR}\rho_0 \int d\mathbf{r}\, \hat{\phi}_A(\mathbf{r})(\hat{\phi}_B(\mathbf{r}) + \hat{\phi}_R(\mathbf{r}))$$

$$H_2[\mathbf{R}] = \chi_{BR}\rho_0 \int d\mathbf{r}\, \hat{\phi}_B(\mathbf{r})\hat{\phi}_R(\mathbf{r}) \quad (6)$$

The above expressions are combined with the condition of incompressibility and are reexpressed as

$$H_1[\mathbf{R}] = -\left(\frac{\chi_{ABR}\rho_0}{4} - \frac{\chi_{BR}\rho_0}{16}\right)\int d\mathbf{r}\, [\hat{\phi}_A(\mathbf{r}) - (\hat{\phi}_B(\mathbf{r}) + \hat{\phi}_R(\mathbf{r}))]^2$$

$$H_2[\mathbf{R}] = -\frac{\chi_{BR}\rho_0}{4}\int d\mathbf{r}\, [\hat{\phi}_B(\mathbf{r}) - \hat{\phi}_R(\mathbf{r})]^2 \quad (7)$$

In the following, we discuss our results with parameter space of the modified interaction parameters, $\chi_1 \equiv \chi_{ABR} - \chi_{BR}/4$ and $\chi_2 \equiv \chi_{BR}$, in terms of which the above equations can be written as:

$$H_1[\mathbf{R}] = -\frac{\chi_1\rho_0}{4}\int d\mathbf{r}\, [\hat{\phi}_A(\mathbf{r}) - (\hat{\phi}_B(\mathbf{r}) + \hat{\phi}_R(\mathbf{r}))]^2$$

$$H_2[\mathbf{R}] = -\frac{\chi_2\rho_0}{4}\int d\mathbf{r}\, [\hat{\phi}_B(\mathbf{r}) - \hat{\phi}_R(\mathbf{r})]^2 \quad (8)$$

Variations in χ_1 (the only interaction effect studied in this article) are assumed to arise from changes in the interaction between A block and combined units of B and R.

(iii) To model the orientational interactions between the rodlike mesogenic units, we utilize a Maier−Saupe type interaction potential. The latter is a mean-field representation where entropic costs arising from nonaligned configurations of rods are ascribed to an energetic cost involving the orientational order parameter $\hat{\mathbf{S}}(\mathbf{r})$ (eq 3). Explicitly,

$$H_3[\mathbf{R}] = -\frac{\mu\rho_0}{2}\int d\mathbf{r}\, \hat{\mathbf{S}}(\mathbf{r}):\hat{\mathbf{S}}(\mathbf{r}) \quad (9)$$

where the Maier−Saupe parameter μ represents the strength of orientational interactions, with high values of μ favoring a stronger alignment of the rods. The above approach for modeling orientational interactions has been shown to provide semiquantitatively accurate results for rod−coil block copolymers even possessing reasonably long rods.[3] For SCLC block copolymer systems, which typically involves much shorter rodlike units, this approximation is expected to be even more accurate in describing the orientational interactions.

In sum, the overall partition function for our model can be written as

$$\mathcal{Z} \propto \int \mathcal{D}\mathbf{R}_\alpha(s)\, d[\mathbf{u}_\alpha(s)]\, \exp[-\beta(H_0 + H_1 + H_2 + H_3)]\delta[\hat{\phi}_A(\mathbf{r}) + \hat{\phi}_B(\mathbf{r}) + \hat{\phi}_R(\mathbf{r}) - 1] \quad (10)$$

Using standard field-theoretic techniques, the quadratic interactions in the Hamiltonian can be decoupled by introducing fluctuating chemical potential fields conjugate to the density and orientational order parameters.[24] In a nondimensional representation, where all lengths are nondimensionalized using the unperturbed radius of gyration $R_g = b(N/6)^{0.5}$, and the contour variables s and p are nondimensionalized using the overall molecular weight N, the partition function can be expressed as a functional integral

$$\mathcal{Z} \propto \int_{-\infty}^{\infty}\mathcal{D}[W_1]\int_{-\infty}^{\infty}\mathcal{D}[W_2]\int_{-\infty}^{\infty}\mathcal{D}[\pi]\int_{-\infty}^{\infty}\mathcal{D}[\mathbf{M}] \times \exp[-\beta H(W_1, W_2, \pi, \mathbf{M})] \quad (11)$$

where

$$H(W_1, W_2, \pi, \mathbf{M}) = -CV \ln \mathcal{Q} + \frac{C}{\chi_1 N}\int d\mathbf{r}\, W_1^2(\mathbf{r}) + \frac{C}{\chi_2 N}\int d\mathbf{r}\, W_2^2(\mathbf{r}) - iC\int dr\pi(\mathbf{r}) + \frac{C}{2\mu N}\int d\mathbf{r}\, \mathbf{M}(\mathbf{r}):\mathbf{M}(\mathbf{r}) \quad (12)$$

In the above expression, $C \equiv \rho_0 R_g^3/N$ and V is the nondimensional system volume. $W_1(\mathbf{r})$ represents the potential field conjugate to the difference in volume fractions of the A and B + R blocks ($\hat{\phi}_A(\mathbf{r}) - (\hat{\phi}_B(\mathbf{r}) + \hat{\phi}_R(\mathbf{r}))$), and $W_2(\mathbf{r})$ represents the potential field conjugate to the difference in volume fractions of B and R components ($\hat{\phi}_B(\mathbf{r}) - \hat{\phi}_R(\mathbf{r})$). The incompressibility is enforced by the pressure like chemical potential field $\pi(\mathbf{r})$.[24] $\mathbf{M}(\mathbf{r})$ is a tensor field conjugate to the orientational order parameter $\hat{\mathbf{S}}(\mathbf{r})$.[3] In the above expression, $\mathcal{Q}$ represents the single chain partition function of a polymer in the external fields $W_1(\mathbf{r})$, $W_2(\mathbf{r})$, $\pi(\mathbf{r})$, and $\mathbf{M}(\mathbf{r})$, and is given by

$$\mathcal{Q}[W_1, W_2, \pi, \mathbf{M}] \propto \int \prod_{\alpha=1}^{\alpha=n} d[\mathbf{u}_\alpha(s)]\, d\mathbf{R}_\alpha(s) \times \exp\left[-\frac{1}{4}\int_0^{f_A+f_B} ds \left(\frac{d\mathbf{R}_\alpha}{ds}\right)^2 - \int_0^{f_A} ds\, (-W_1(\mathbf{R}_\alpha(s)) + i\pi(\mathbf{R}_\alpha(s))) - \int_{f_A}^{f_A+f_B} ds\, (W_1(\mathbf{R}_\alpha(s)) - W_2(\mathbf{R}_\alpha(s)) + i\pi(\mathbf{R}_\alpha(s))) - \int dr\, (W_1(\mathbf{r}) - W_2(\mathbf{r}) + i\pi(\mathbf{r}))\hat{\phi}_R(\mathbf{r}) + \int d\mathbf{r}\, \mathbf{M}(\mathbf{r}):\hat{\mathbf{S}}(\mathbf{r})\right] \quad (13)$$

We denote the potential fields acting on A, B, and R segments as $W_A(\mathbf{r})$, $W_B(\mathbf{r})$, and $W_R(\mathbf{r})$ respectively, and are in turn related to the $W_1(\mathbf{r})$, $W_2(\mathbf{r})$, and $\pi(\mathbf{r})$ fields as

$$W_A(\mathbf{r}) = -W_1(\mathbf{r}) + i\pi(\mathbf{r})$$
$$W_B(\mathbf{r}) = W_1(\mathbf{r}) - W_2(\mathbf{r}) + i\pi(\mathbf{r})$$
$$W_R(\mathbf{r}) = W_1(\mathbf{r}) + W_2(\mathbf{r}) + i\pi(\mathbf{r}) \quad (14)$$

We observe that eq 13 can be simplified by noting that the orientational degrees of freedom of each of the rod units on the backbone are independent of each other. This allows us to express eq 13 as

$$\mathcal{Q} \propto \int d\mathbf{R}_\alpha \exp\left[-\frac{1}{4}\int_0^{f_A+f_B} ds \left(\frac{d\mathbf{R}_\alpha}{ds}\right)^2 - \int_0^{f_A} ds\, W_A(\mathbf{R}_\alpha) - \int_{f_A}^{f_A+f_B} ds\, W_B(\mathbf{R}_\alpha) + N\int_{f_A}^{f_A+f_B} ds \ln \mathcal{G}(\mathbf{R}_\alpha)\right] \quad (15)$$

where

$$\mathcal{G}(\mathbf{r}) = \int d\mathbf{u} \exp\left[-\int_0^{f_R/N_R} dp \left(W_R(\mathbf{r} + \beta p\mathbf{u}) - \mathbf{M}(\mathbf{r} + \beta p\mathbf{u}):\left(\mathbf{uu} - \frac{\mathbf{I}}{3}\right)\right)\right] \quad (16)$$

In the above representation, $\ln \mathcal{G}(\mathbf{r})$ can be construed as a pseudo "effective potential" acting on a monomer of the B block at position $\mathbf{r}$ arising due to the statistical weight of the rod units linked to it. In the above equation, $\beta(\equiv aN/b(N/6)^{1/2})$ is the nondimensional parameter characterizing the length of a rod block.

We observe that the expression eq 15 for the partition function of a single polymer chain resembles the partition function for a flexible diblock copolymer, with an overall chemical potential acting on the B segments which includes the rod contributions: $W_B^*(\mathbf{r}) = W_B(\mathbf{r}) - N \ln \mathcal{G}(\mathbf{r})$. Moreover, since $\mathcal{G}(\mathbf{r})$ involves only an integral over $\mathbf{u}$, eq 16 can be evaluated using straightforward numerical techniques. Consequently, the above single chain partition function (eq 15) can be evaluated by solving diffusion-like equations for the end-segment distribution functions,[24,25] which are very similar in structure to that of a flexible diblock copolymer. Explicitly, if $q(\mathbf{r}, s)$ represents the statistical weight for a chain of length "s" to have its end at position $\mathbf{r}$

$$\frac{\partial}{\partial s} q(\mathbf{r}, s) = \begin{cases} \nabla^2 q(\mathbf{r}, s) - W_A(\mathbf{r}) q(\mathbf{r}, s) & 0 \le s \le f_A \\ \nabla^2 q(\mathbf{r}, s) - W_B^*(\mathbf{r}) q(\mathbf{r}, s) & f_A \le s \le f_A + f_B \end{cases} \quad (17)$$

In terms of $q(\mathbf{r}, s)$, we have

$$\mathcal{Q} = \frac{1}{V}\int d\mathbf{r}\, q(\mathbf{r}, f_A + f_B) \quad (18)$$

While all our developments so far are exact, except insofar as the approximations inherent in the micromechanical representation, we now invoke the mean-field approximation, wherein the partition function ($\mathcal{Z}$) is approximated by evaluating the functional integral at its saddle point.[24,26] This leads to a set of equations relating the potential fields $W_1(\mathbf{r})$, $W_2(\mathbf{r})$, $\pi(\mathbf{r})$, and M($\mathbf{r}$) and the species volume fractions and orientational order parameter $\phi_A(\mathbf{r})$, $\phi_B(\mathbf{r})$, $\phi_R(\mathbf{r})$, and $\mathbf{S}(\mathbf{r})$ to be solved in a self-consistent manner. Explicitly, the self-consistent equations are

$$\frac{2}{\chi_1 N} W_1(\mathbf{r}) = \phi_A(\mathbf{r}) - [\phi_B(\mathbf{r}) + \phi_R(\mathbf{r})]$$
$$\frac{2}{\chi_2 N} W_2(\mathbf{r}) = \phi_B(\mathbf{r}) - \phi_R(\mathbf{r})$$
$$\phi_A(\mathbf{r}) + \phi_B(\mathbf{r}) + \phi_R(\mathbf{r}) = 1$$
$$\frac{1}{\mu N}\mathbf{M}(\mathbf{r}) = \mathbf{S}(\mathbf{r}) \quad (19)$$

In the above expression, $\phi_i(\mathbf{r})$ represents the local volume fractions of the different components, while $\mathbf{S}(\mathbf{r})$ is the local orientational order parameter. The local volume fractions of the flexible components can be calculated in a manner similar to the situation of pure flexible diblock copolymers:[1]

$$\phi_A(\mathbf{r}) = \frac{1}{\mathcal{Z}}\int_0^{f_A} ds\, q(\mathbf{r}, s) q^\dagger(\mathbf{r}, f_A + f_B - s)$$
$$\phi_B(\mathbf{r}) = \frac{1}{\mathcal{Z}}\int_{f_A}^{f_A+f_B} ds\, q(\mathbf{r}, s) q^\dagger(\mathbf{r}, f_A + f_B - s) \quad (20)$$

In the above equations, $q^\dagger(\mathbf{r}, s)$ is the end-segment distribution function and represents the statistical weight for a chain of length "s" to have its end at position at $\mathbf{r}$. It is defined in the same way as $q(\mathbf{r}, s)$, except that s is measured from the end of B-block, and satisfies

$$\frac{\partial}{\partial s} q^\dagger(\mathbf{r}, s) = \begin{cases} \nabla^2 q^\dagger(\mathbf{r}, s) - W^*{}_B(\mathbf{r}) q^\dagger(\mathbf{r}, s) & 0 \le s \le f_B \\ \nabla^2 q^\dagger(\mathbf{r}, s) - W_A(\mathbf{r}) q^\dagger(\mathbf{r}, s) & f_B \le s \le f_A + f_B \end{cases} \quad (21)$$

The volume fractions and orientational order parameters of the rod units can be obtained as

$$\phi_R(\mathbf{r}) = N \int d\mathbf{u} \int_0^{f_R/N_R} dp \frac{\phi_B(\mathbf{r} - \beta p\mathbf{u})}{\mathscr{J}(\mathbf{r} - \beta p\mathbf{u})} \times \exp\left[- \int_0^{f_R/N_R} dp' \left(W_R(\mathbf{r} - \beta p\mathbf{u} + \beta p'\mathbf{u}) - \mathbf{M}(\mathbf{r} - \beta p\mathbf{u} + \beta p'\mathbf{u}) : \left(\mathbf{uu} - \frac{\mathbf{I}}{3} \right) \right) \right] \quad (22)$$

and

$$\mathbf{S}(\mathbf{r}) = N \int d\mathbf{u} \int_0^{f_R/N_R} dp \frac{\phi_B(\mathbf{r} - \beta p\mathbf{u})}{\mathscr{J}(\mathbf{r} - \beta p\mathbf{u})} \left(\mathbf{uu} - \frac{\mathbf{I}}{3} \right) \times \exp\left[- \int_0^{f_R/N_R} dp' \left(W_R(\mathbf{r} - \beta p\mathbf{u} + \beta p'\mathbf{u}) - \mathbf{M}(\mathbf{r} - \beta p\mathbf{u} + \beta p'\mathbf{u}) : \left(\mathbf{uu} - \frac{\mathbf{I}}{3} \right) \right) \right] \quad (23)$$

The physical interpretation of the above two expressions is that the density (or the orientational density parameter) of the rod segment "p" at position $\mathbf{r}$ and oriented at an angle $\mathbf{u}$, is directly linked to the density of backbone ($\phi_B(\mathbf{r})$) at the position $\mathbf{r} - \beta p\mathbf{u}$. The integrals in the above equations then accounts for all the possible orientation of the rods and all the monomers of the rod, with the exponential terms accounting for the probability that a rod segment whose link with the flexible backbone located at $\mathbf{r} - \beta p\mathbf{u}$ is oriented at an angle $\mathbf{u}$.

In essence, our model formulation transforms the influence of side chain units as a potential onto the B segments, necessitating solution of only two diffusion equations ($q(\mathbf{r}, s)$ and $q^\dagger(\mathbf{r}, s)$) for the polymer. This contrasts with earlier models of comb-like polymer where the combs were assumed to be grafted at arbitrary locations and requires solution of multiple diffusion equations.[17]

A. Details of Numerical Calculations and Parameters. The self-consistent equations (eq 19) are solved by a real space evolution method developed by Fredrickson and co-workers.[24] This method entails starting with random initial conditions for the potential fields, which are then evolved until the self-consistent solutions to eq 18 are achieved. The pseudo evolution equations employed in this scheme are of the following form:

$$\frac{\partial W_1(\mathbf{r})}{\partial t} = -\lambda_{W_1} \left(\frac{2}{\chi_1 N} W_1(\mathbf{r}) - [\phi_A(\mathbf{r}) - (\phi_B(\mathbf{r}) + \phi_R(\mathbf{r}))] \right)$$

$$\frac{\partial W_2(\mathbf{r})}{\partial t} = -\lambda_{W_2} \left(\frac{2}{\chi_2 N} W_2(\mathbf{r}) - [\phi_B(\mathbf{r}) - \phi_R(\mathbf{r})] \right)$$

$$\frac{\partial \pi(\mathbf{r})}{\partial t} = \lambda_\pi [1 - \phi_A(\mathbf{r}) - \phi_B(\mathbf{r}) - \phi_R(\mathbf{r})]$$

$$\frac{\partial \mathbf{M}(\mathbf{r})}{\partial t} = -\lambda_M \left(\frac{\mathbf{M}(\mathbf{r})}{\mu N} - \mathbf{S}(\mathbf{r}) \right) \quad (24)$$

In the above equations, the fictitious mobility coefficients (λ_π) for the incompressibility field $\pi(\mathbf{r})$ was typically chosen as between 0.2 and 0.3, and the mobility coefficients (λ_{W_1}, λ_{W_2}, and λ_M) for other fields were chosen to be between 0.1 and 0.15. We employed a box size of $8R_g \times 8R_g$ for our simulations. The discretization along the length of flexible backbone Δs was chosen to be 0.005. The diffusion equations in two dimensions were solved by an operator splitting strategy.[27] Despite the fact that simulations were carried out assuming two-dimensional variations in volume fractions and orientational order parameter, the orientational vector was allowed to be a unit vector in the three-dimensional plane. Hence the average orientational order parameter $\mathbf{S}(\mathbf{r})$ and its conjugate potential field $\mathbf{M}(\mathbf{r})$, are symmetric, traceless 3×3 matrices. Integrations over orientational vector $\mathbf{u}(\mathbf{r})$ were evaluated by utilizing a 10-point Gaussian quadrature.[27]

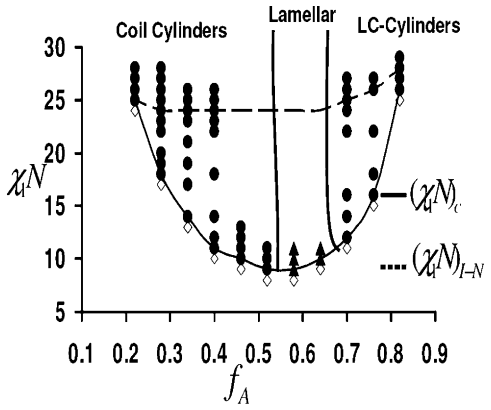

Figure 2. Self-assembly phase diagram obtained from 2D calculations. The parameters are $N = 200$ and $m = 5$. The solid line represents the transition from disordered phase to microphase separation, and the dashed line represents the transition to smectic ordering. Open diamonds represents disordered phase, while triangles represent lamellar phases and the circles represent the cylindrical morphologies discussed in the text.

The overall self-assembly behavior is governed by a vast parametric space which includes f_A, $\chi_1 N$, $\chi_2 N$, N_R, m, μN, and β. The first two parameters also arise in the context of the phase behavior of the flexible diblock copolymers, while the other parameters arise in the specific context of the SCLC block copolymer. In the results discussed in the next section, the ratio $\mu N/\chi_1 N$ was kept fixed at a value of 15. The nondimensional length of the rod unit was fixed at $\beta = 5$ for the case of higher molecular weight. The interaction parameter between the flexible backbone and the side chain mesogenic units was also kept fixed throughout the simulations as $\chi_2 N = 20$.

To determine the onset and characteristics of microphase separation transition, both the equilibrium component volume fraction profiles and the free energies are used. To identify the orientational ordering transition, we calculate an order parameter: $\bar{S}(\mathbf{r}) = 1.5\lambda_{max}(\mathbf{r})$, where $\lambda_{max}(\mathbf{r})$ denotes the maximum eigenvalue of the tensor $\mathbf{S}(\mathbf{r})$. This order parameter, when normalized by rod volume fraction $\phi_R(\mathbf{r})$ equals unity for the case of complete alignment of the rods, and is zero for random orientation of rods. The orientation of the rod units are along the eigenvector corresponding to the maximum eigenvalue of the orientational order tensor ($\lambda_{max}(\mathbf{r})$). In the following section, we present results obtained by assuming that the solutions of the self-consistent field theory equations exhibit a 2-D symmetry.

III. Results and Discussion

A. Phase Diagram and Morphologies. In the present section, we present results which show the effects of varying the volume fraction of A block (f_A) and the interaction parameter ($\chi_1 N$) on the nature of morphologies formed and the orientational ordering of the mesogenic units. In Figure 2, we present the self-assembly phase diagram for the case of $N = 200$ and $m = 5$. The boundaries indicated between the different phases are just meant to be guidelines to the eye and do not represent real phase boundaries obtained as output of our simulations. The solid line represents the transition from isotropic to phase separated morphology (denoted as $(\chi_1 N)_C$), and the dashed line represents the onset of orientational ordering of the mesogenic units (denoted as $(\chi_1 N)_{I-N}$). From Figure 2, it can be observed that

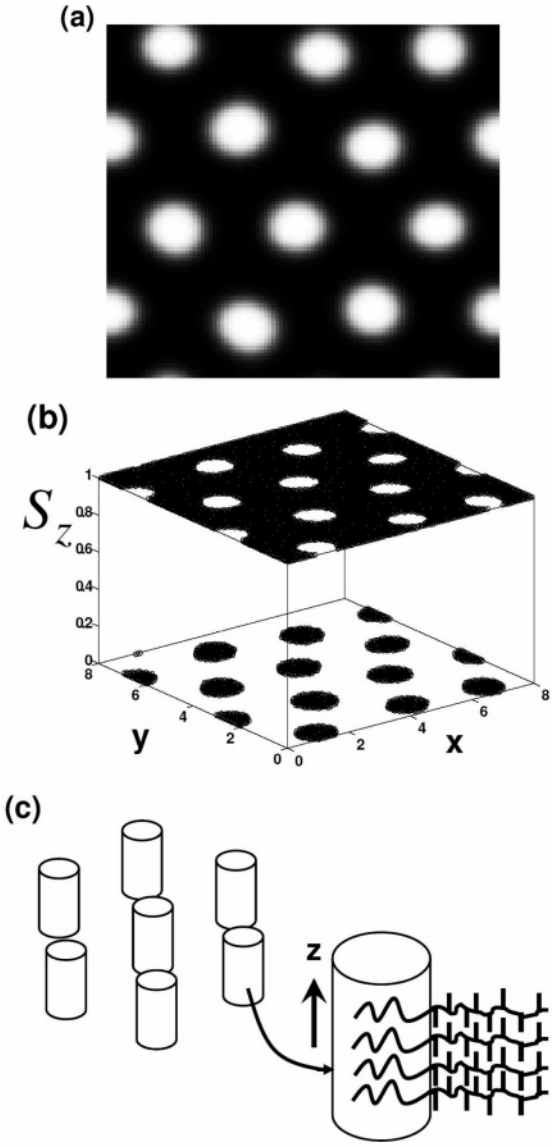

Figure 3. (a) Hexagonally packed coil cylinders in a continuous LC block phase. $N = 200$, $m = 5$, $f_A = 0.22$ and $\chi_1 N = 25$. (b) The *z*-component ($\mathbf{S}_z(\mathbf{r})$) of the eigenvector corresponding to $\lambda_{max}(\mathbf{r})$. In regions where LC phase appears, the value of $\mathbf{S}_z(\mathbf{r})$ is 1.0, which implies that the orientation is along the *z*-axis. (c) Schematic representation for this morphology.

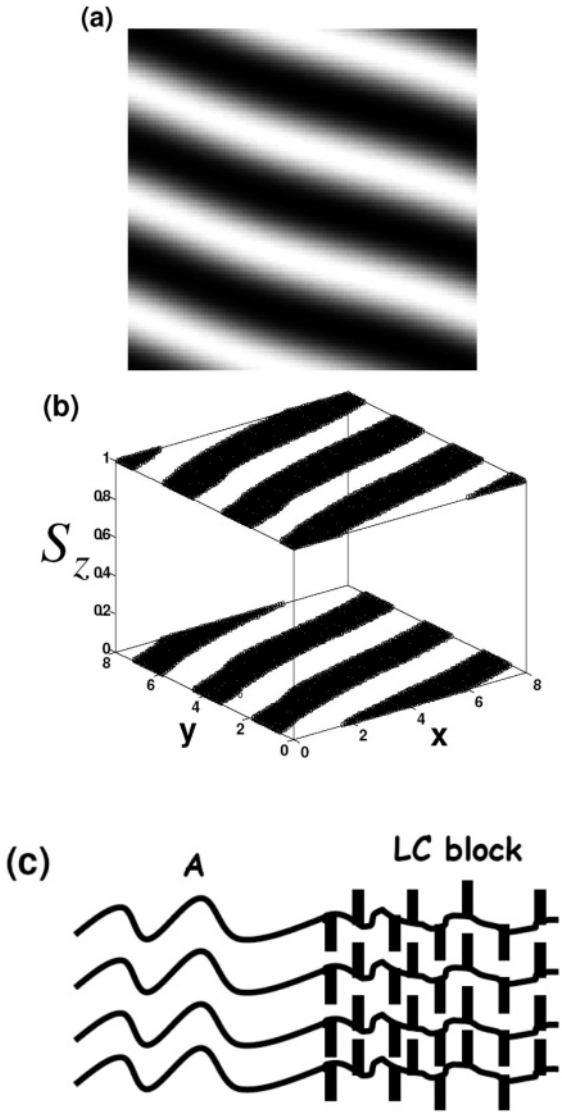

Figure 4. (a) Lamellar morphology for amorphous and LC blocks. The parameters are $N = 200$, $m = 5$, $f_A = 0.64$ and $\chi N = 10$. The rods are oriented parallel to interface between the two blocks. (b) Plot of the z-component ($\mathbf{S}_z(\mathbf{r})$) of the eigenvector corresponding to $\lambda_{max}(\mathbf{r})$. In regions where the LC phase appears, the orientation is along the *z*-axis. (c) Schematic representing microphase separation and orientational ordering.

the critical value of the Flory−Huggins interaction parameter $(\chi_1 N)_C$ needed for microphase separation transition is less than or equal to the value of $(\chi_1 N)_{I-N}$ for the onset of smectic ordering, suggesting that the formation of microphases was a necessary condition for the development of orientational ordering. Overall, we also observe that the phase diagram is not symmetric in the volume fractions of the A and B blocks.

At low volume fractions of the A block ($0.22 \leq f_A \leq 0.52$), hexagonally packed cylinders of A phase surrounded by continuous matrix of LC (B + R) block are formed. Figure 3(a) displays a representative 2D volume fraction profile (in the x-y plane) for such a morphology. In Figure 3b, the z-component ($\mathbf{S}_z(\mathbf{r})$) of the eigenvector corresponding to the orientation is displayed. From Figure 3b, it is evident that in the region outside the cylinder (B + R phase), the value of $\mathbf{S}_z(\mathbf{r})$ is unity, which implies that the rods prefer to orient themselves along the axis of coil cylindrical domains. The schematic shown in Figure 3c depicts the conformations of the chains and the orientational arrangement of side chain units outside the cylindrical domains. The flexible backbone stretches outward from the curved interface, thus aligning the side chain units along the axis of the cylinder. This orientation can be rationalized by observing that the alternative, involving the tangential orientation of the mesogens around the cylindrical domains would lead to defects and would be unfavorable relative to the observed axial orientation of the rods. Experimental observations of this morphology and the predicted orientation of the rods (Figure 3c) have been reported by many independent researchers.[9,10,12−14]

In the intermediate region of the phase diagram ($0.52 \leq f_A \leq 0.64$), lamellar phases of amorphous and LC blocks are observed in conjunction with an orientational ordering within the lamellar domains. Figure 4(a) displays the 2-D density profile for lamellar structure observed at a volume fraction of $f_A = 0.64$ and $\chi_1 N = 10$. In Figure 4b, the z-component ($\mathbf{S}_z(\mathbf{r})$) of the eigenvector corresponding to the orientation is displayed. In the region of LC phase (B + R), the value of $\mathbf{S}_z(\mathbf{r})$ is unity, suggesting that the rod units are aligned parallel to the block copolymer interface and out of the plane of the paper. Figure 4c shows a schematic of the chain conformations and the

orientation of rods within the lamellar microphases. This orientation can be rationalized as arising from the tendency of the flexible backbone (B segments) to stretch outward from the interface, thus aligning the side-chain mesogenic units in the direction parallel to the block copolymer interface. The results of Figure 4 are also consistent with experimental observations which have reported such morphologies and orientations for SCLC block copolymers with a short alkyl spacers.[15] In the case of a simple flexible diblock copolymer, lamellar phases are typically observed in the center of the phase diagram ($0.35 \lesssim f_A \lesssim 0.65$). In contrast, we observe for the case of side-chain liquid crystalline block copolymers, that lamellar phases are formed at values of f_A slightly greater than 0.5. This asymmetry in the phase diagram can be ascribed to the fact that the attachment of the rod units renders the LC block much more bulkier than the amorphous coil block. Consequently even a volume fraction of $f_A = 0.5$ involves an asymmetric diblock copolymer with $N_A > N_R$ (i.e., N_B), thereby favoring curved phases. Since the effective volume fractions of A and the B + R blocks are the same, in this scenario, the shorter block (i.e., the B unit) tends to favor being on the outside of the cylinders. Hence, cylindrical domains of amorphous coil blocks are observed in the regime of the phase diagram where the volume fraction f_A is close to and even greater than 0.5.

At values of the volume fraction of the A block corresponding to the majority phase ($0.7 \leq f_A \leq 0.82$), we observe hexagonal phases where the LC block is confined in a cylindrical morphology within a continuous matrix of flexible A block. In Figure 5a, we present representative volume fraction profiles for such hexagonally packed LC cylinders for $\chi_1 N = 18$ and $f_A = 0.76$. In Figure 5b, we present a 3D plot of $\mathbf{S}_z(\mathbf{r})$, which is the z-component of the normalized eigenvector corresponding to $\lambda_{max}(\mathbf{r})$. If the variations in the density profile are assumed to be in the $x-y$ plane, then the orientation of the rod units are observed to be along the z-axis, i.e., the axis of the cylindrical domains. A schematic of this hypothesized conformations of the chains and the orientational characteristics of the rods are depicted in Figure 5c. In this arrangement, the flexible backbone (B) is stretched away from the curved block copolymer interface to minimize contacts between A units and B + R units. Within the cylindrical domains, the rod units have the option of either orienting tangential to the interface or in the axial direction. However, a tangential orientation inside the cylindrical domains is expected to lead to significant energy costs due to defects, and is unfavorable relative to the observed axial orientation of the rods. Experimental observations of such LC cylinder morphologies are reported by Ober and co-workers for a volume fraction of the coil block at $f_A = 0.78$.[9] They have also speculated that the smectic ordering within the cylindrical domains will be similar to the manner depicted in the schematic shown in Figure 5c. It is pertinent to note that by assuming 2D variations in composition profiles we preclude observation of profiles which involve phase separation between the rods (R) and the backbone coils (B).

In sum, the above morphologies are observed to be a combination of morphologies observed for flexible diblock copolymers along with orientational ordering of the rod units. On the other hand, these morphologies differ significantly from that observed in rod−coil copolymers, wherein, due to more severe steric constraints, mainly lamellar-like morphologies are observed. Moreover, in all our results we observed that microphase separation (ODT) was necessary for development of orientational ordering (I−N), which is also consistent with experimental results wherein it has been observed that well-

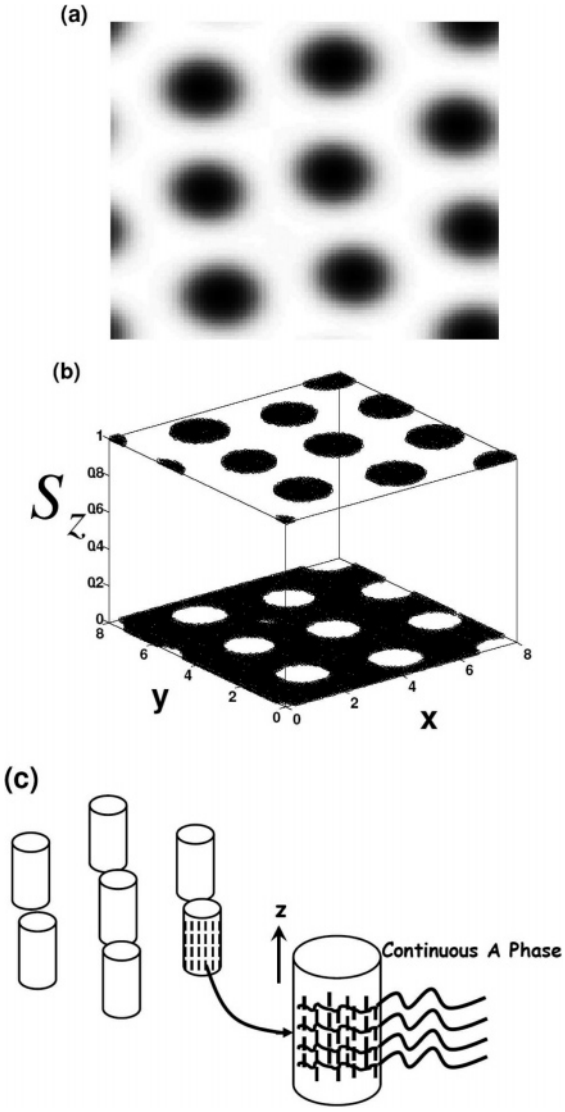

Figure 5. (a) Hexagonally packed LC cylinders in a matrix of A block. The parameters are $N = 200$, $m = 5$, $f_A = 0.76$ and $\chi_1 N = 18$. (b) Plot of the z-component ($\mathbf{S}_z(\mathbf{r})$) of the eigenvector corresponding to λ_{max}-($\mathbf{r}$). In regions where the LC phase appears, the orientation is along the z-axis. (c) Schematic representation of the observed morphology.

defined lamellae microphase was required to stabilize the formation of smectic C phase.[15] In contrast, in rod−coil copolymers a precursor nematic phase was typically observed prior to microphase separation.[28] The absence of such a precursor disordered nematic phase for SCLC block copolymers can be rationalized as due to the shorter length and lower volume fraction of rod units. Consistent with this hypothesis, the value of averaged orientational order parameter ($\langle\bar{S}(\mathbf{r})\rangle$) at the I−N transition was typically found to be in the range 0.2−0.5, much lower than the values observed for rod−coil block copolymers.[3]

B. Effect of Molecular Weight. We briefly discuss the effect of molecular weight N on the above morphologies by comparing the transition lines for the cases of $N = 100$ and $N = 200$ for a fixed value of rod length ($m = 5$) in Figures 6a and b. Overall, for both the molecular weights we observe that the system exhibits similar kinds of morphologies in similar ranges of volume fractions. For the case of smaller N, the transition for smectic ordering ($(\chi_1 N)_{I-N}$) is seen to move downward and even coincide with the microphase separation transition ($\chi_1 N)_C$ at very low volume fractions of coil. We note that this behavior is consistent with the experiments of Zheng and co-workers who had observed that for lower molecular weights and higher LC

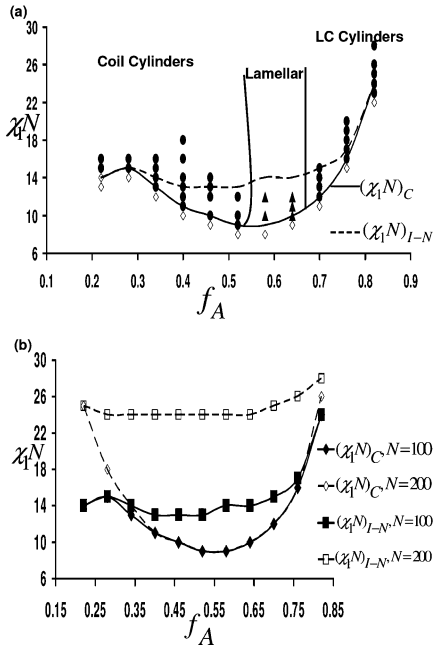

Figure 6. (a) Self-assembly phase diagram obtained from 2D calculations for the parameters are $N = 100$ and $m = 5$. Microphase separation and isotropic−smectic transition occurred at the same value of $\chi_1 N$ for this parametric case. (b) Comparison of microphase separation transition and isotropic−nematic transition (I−N) of the rods units for two cases: $N = 200$ and $m = 5$, and $N = 100$ and $m = 5$.

block volume fractions, the ODT coincided with the I−N transition temperature.[7] To rationalize this decrease in the critical $(\chi_1 N)_{\mathrm{I-N}}$ for orientational ordering, we note that whereas the onset of microphase separation is governed by value of $\chi_1 N$, the onset of orientational ordering can be understood to be governed by the Maier−Saupe parameter μ (for a fixed length of the rod m − cf. discussion following eq 27). The ease of undergoing orientational ordering relative to microphase separation is thus governed by the factor $\mu/\chi_1 N$. For the present case, since the ratio μ/χ_1 is kept fixed, the orientational ordering relative to the microphase separation is governed by the factor $1/N$. Hence, on decreasing N, the orientational ordering is seen to be favored. We also observe that for $N = 100$, at lower volume fractions of the coil block ($0.22 \leq f_{\mathrm{A}} \leq 0.28$), the earlier onset of orientational ordering also drives the ODT to lower values of $\chi_1 N$. As more explicitly demonstrated in our SST model, for the parametrization adopted in this article the effective repulsion between the coil and LC blocks depend on the orientational order parameter (cf. Section IVB). Consequently, a nonzero value of the orientational order parameter renders the effective repulsion stronger and hence lowers $(\chi_1 N)_{\mathrm{C}}$.

C. Summary of Results from Other Parametric Studies. We also determined the effects of using different values for the rod lengths ($m = 3$, 9, and 11) and Maier−Saupe parameters ($\mu/\chi_1 = 10$) upon the phase diagram (in each individual case the remaining parameters were fixed at values corresponding to Figure 2). In all cases, the results obtained could be understood in an intuitive manner (and more explicitly through the SST model presented next section), and hence, we restrict ourselves to a brief discussion of our findings. For all the cases examined, microphase separation transition was found to be a necessary condition for the occurrence of I−N transitions. Overall, the self-assembly morphologies and the order−order transitions were only slightly influenced by parameters such as m and μ. Moreover, except for small values of f_{A}, the microphase separation transition temperature ($(\chi_1 N)_{\mathrm{C}}$) was only weakly affected by the values of the rod length m and the Maier−Saupe parameter μ. In contrast, the orientational ordering transition ($(\chi_1 N)_{\mathrm{I-N}}$) was observed to monotonically decrease upon increasing either the length of the rod block and/or Maier−Saupe parameter. The stronger tendency for orientational ordering can be rationalized as arising from the stronger excluded volume interactions and the more pronounced tendency to orient in longer rods and/or for stronger interactions. In contrast, since in majority of the phase diagram microphase separation transition occurred when the rod units were still in the isotropic phase, and such a transition was much less influenced by the rod length.

IV. Strong Segregation Theory for Ordering in SCLC Block Copolymers

We note that strong segregation theories (SST) have played an important role in the theoretical descriptions of morphologies observed in multicomponent polymeric materials.[1,21,22,29] The results presented in the preceding section suggested that morphologies observed in SCLC parallels those observed in flexible diblock copolymers, except with the additional possibility of orientational ordering within the mesophases. These results motivated us to examine whether a SST approach can be developed for predicting the morphologies observed in SCLC.

A. Model and Governing Equations. To enable a SST development, we distill the model and physics of self-assembly in SCLC polymers into a few key features and assumptions: (i) The rod units are assumed to contribute to an increased monomeric volume of the B segments. In turn, the latter affects the interfacial tension of AB interphases. (ii) The effective interaction between A and B blocks depends upon the orientational order parameter in the corresponding phase. (iii) The orientational ordering of the rod mesophases can be discerned by adopting the classical Maier−Saupe theory adopted to account for the volume fraction of rods in the mesophase. (iv) As always, SST is expected to be valid only for the situation of strongly segregated phases wherein the interfacial thickness is small.[20] In section IVC, we discuss some limitations of these model assumptions.

Our approach involves an estimation of the free energies of: (a) disordered−isotropic, (b) disordered−nematic, (c) ordered−isotropic, and (d) ordered−nematic phases to determine the preferred phase. In SST, all free energies are evaluated either for a compositionally homogeneous state or a completely segregated state. In either case, estimation of the effective volume fractions and the enthalpic interactions prove straightforward. For ordered phases, the additional free energy contributions arising from the interfacial tension and stretching free energies have been evaluated for flexible diblock copolymers and can be adapted to our context.

a. Isotropic—Nematic Transitions. Among the different possible phases, the transitions between the isotropic and nematic phases (in both the disordered and ordered regimes) are governed only by the Maier−Saupe parameter μ and the effective rod volume fractions in that phase. Explicitly, in the Maier−Saupe approximation the orientational free energy can be expressed on a *per rod basis* as[30]

$$\beta F_{\mathrm{orient}} = \int \mathrm{d}\theta\, f(\theta) \ln[f(\theta)] \sin\theta - \frac{m\mu\phi_{\mathrm{R}}}{2} S^2 \qquad (25)$$

where $f(\theta)$ denotes the angular distribution of the rod orientations and normalized such that

$$\int \mathrm{d}\theta\, f(\theta) \sin\theta = 1 \qquad (26)$$

and

$$S = \int \mathrm{d}\theta\, f(\theta) P_2(\cos\theta) \sin\theta \tag{27}$$

where $P_2(x)$ denotes the Legendre polynomial of second order. Minimizing over $f(\theta)$ yields a first-order phase transition between an isotropic and nematic phase at

$$(m\mu\phi_R)_C = 4.541 \tag{28}$$

The effective volume fractions of the rods can be estimated in the disordered and ordered phases as $\phi_R^D = m(1 - f_A)/(m + 1)$ and $\phi_R^O = m/(m + 1)$ respectively. Whence, for a given χ_1 (recall that our parametrization fixes the ratio μ/χ_1), the relative preference (within either a disordered or ordered phase) for an isotropic vs nematic phase and the respective orientational order parameters can be evaluated a priori by checking if $m\mu(\phi_R^D, \phi_R^O) > 4.541$ and subsequently minimizing the above functional eq 25 to determine the order parameter within that phase. Subsequently, to discern the order−disorder transition (ODT) it just suffices to compare the free energies of an ordered and a disordered phase with *predetermined* orientational ordered parameters S_O and S_D, respectively.

b. Order—Disorder Transitions. To determine the order disorder transitions we adopt many of the earlier developments in the context of flexible diblock copolymers, while making allowance for the possible difference in free energies due to the differences in order parameters S_O and S_D. We use a model of a flexible A-BR block copolymer containing N segments with the segmental volume of the A units ρ_0^{-1} and the segmental volume of the BR units $(m + 1)\rho_0^{-1}$. The volumes of A block (V_A), BR block (V_{BR}), and the entire copolymer chain V_C are

$$V_A = \frac{N_A}{\rho_0}; \quad V_{BR} = \frac{N_R(m+1)}{\rho_0}; \quad V_C = V_A + V_{BR} \tag{29}$$

The unperturbed radius of gyration of A, B, and the total chain are

$$(R_g^2)_A = \frac{N_A b^2}{6}; \quad (R_g^2)_B = \frac{N_R b^2}{6}; \quad (R_g^2)_C = \frac{(N_A + N_R)b^2}{6} = \frac{b^2 N}{6}\frac{1 + mf_A}{1 + m} \tag{30}$$

Hence, the copolymer chain may be viewed as a flexible Gaussian chain of $N(1 + mf_A)/(1 + m)$ effective monomers.

The difference in free energies between the ordered and disordered phases are expressed as

$$\frac{(F^{ord} - F^{dis})}{k_B T} = \Delta F_{bulk} + F_{int} + F_{elastic} \tag{31}$$

In the above, ΔF_{bulk} denotes the bulk free energy difference between the ordered and disordered phases, F_{int} and $F_{elastic}$ represents the interfacial and elastic free energy costs in the ordered phases. ΔF_{bulk} can be estimated as (on a per chain basis):

$$\Delta F_{bulk} = -f_A(1 - f_A)\chi_1 N + \frac{\mu m^2 N}{2(m+1)^2}(1 - f_A)[(1 - f_A)S_D^2 - S_O^2] + \frac{N(1 - f_A)}{m + 1}[\sigma(S_D) - \sigma(S_O)] \tag{32}$$

In the above, the first term arises from the enthalpic contributions due to repulsions between A and (B + R) segments. The second term represents the difference in the Maier−Saupe interactions due to a possible difference in the orientational order parameter between the disordered and ordered phases. The third term represents the orientational entropy of the rods in the different phases, with

$$\sigma = \int \mathrm{d}\theta\, f(\theta) \ln[f(\theta)] \sin\theta \tag{33}$$

[The last two terms in eq 32 are identical to those in eq 25]. It is evident from the first two terms of eq 32 that the effective repulsions between the A and BR blocks are dependent upon the value of the orientational order parameter S. This feature can be seen more clearly by noting that the enthalpic contributions to the bulk free energy in our model is of the form:

$$\rho_0^{-1} F_{bulk}^{enth} = -\frac{\chi_1}{4}[\phi_A - (\phi_B + \phi_R)^2] - \frac{\mu}{2}\phi_R^2 S^2 \tag{34}$$

In the approximation used in the SST model, $\phi_R = m\phi_B = m(1 - \phi_A)/(m + 1)$. This allows us to rewrite eq 34 as

$$\rho_0^{-1} F_{bulk}^{enth} = -\left(\frac{\chi_1}{4} + \frac{\mu m^2}{8(m+1)^2} S^2\right)[\phi_A - (\phi_B + \phi_R)^2] + \text{other terms} \tag{35}$$

rendering more clearly that the repulsions between A and BR blocks are governed by an effective interaction parameter χ_{eff}

$$\chi_{eff} = \frac{\chi_1}{4} + \frac{\mu m^2}{8(m+1)^2} S^2 \tag{36}$$

To estimate F_{int} we rely on our model of a conformationally asymmetric diblock copolymer for which Helfand and Sapse have computed the interfacial tension.[29] Explicitly, the interfacial tension γ_{ABR} for a conformationally asymmetric diblock copolymer with monomeric densities ρ_0 and $(m + 1)^{-1}\rho_0$ with an effective interaction parameter χ_{eff} is given as

$$\frac{\beta\gamma_{ABR}}{\rho_0 b} = \sqrt{\frac{\chi_{eff}}{6}}\frac{2[(m+1)^{3/2} - 1]}{3m(m+1)} \tag{37}$$

Strictly speaking, the above expression is only approximate for our situation where the inhomogeneous variations in the orientational order parameter S is also expected to influence the interfacial tension between the phases. The latter is an effect not accounted within our SST model.

To estimate the elastic energy contribution $F_{elastic}$ (and the area per chain required to compute F_{int} from eq 37) requires us to consider different possibilities for ordered phases. In line with our SCFT calculations, we restrict our consideration to the cases of lamellar structures, A-cylinders and BR cylinders. For each of these situations, we adapt the calculations of $F_{elastic}$ presented by Semenov.[21]

(i) Lamellar Phases. For a lamellar phase of period $2h$, the thicknesses of A and BR brushes can be estimated as $h_A = f_A h$ and $h_{BR} = (1 - f_A)h$. The stretching free energy per chain in this configuration is

$$F_{elastic} = \frac{h^2}{4(R_g^C)^2}\left(\frac{f_A(mf_A + 1)}{(m+1)} + (1 - f_A)(mf_A + 1)\right) \tag{38}$$

The interfacial area per chain is, $(N_A + N_R(m+1))/\rho_0 h$, which yields

$$F_{int} = \frac{2(1-\sqrt{1+m}+m(2+m))\sqrt{\chi_{eff}N}}{3m\sqrt{1+m}\sqrt{1+mf_A}}\frac{R_g^C}{h} \quad (39)$$

(ii) Cylindrical Phases. The free energy (per chain) of a *convex* molten cylindrical brush made of a polymer with N_x monomers and with inner radius R_i and outer radius R_o is[21]

$$F_{out}^{cyl} = \frac{3(R_o^2 - R_i^2)\log(R_o/R_i)}{4b^2N_x} \quad (40)$$

The free energy (per chain) of a *concave* molten cylindrical brush made of a polymer with N_x monomers and a radius R_i is

$$F_{in}^{cyl} = \frac{\pi^2}{16b^2}\frac{R_i^2}{N_x} \quad (41)$$

(a) A Cylinders. For cylindrical structures with A chains forming the internal phase of the cylinder with a radius R_i, the thickness of the external (BR phase) cylinder (i.e., $R_o - R_i$ above) can be estimated as $R_i/\sqrt{f_A}$. The interfacial area per chain is as follows: $2f_AN/\rho_0R_i$.

(b) BR Cylinders. For cylindrical structures with BR chains forming the internal phase of the cylinder with a radius R_i, the thickness of the external (A phase) cylinder (i.e., $R_o - R_i$ above) can be estimated as $R_i/\sqrt{1-f_A}$. The interfacial area per chain is: $2(1-f_A)N/\rho_0R_i$.

The sum total of elastic and interfacial free energy costs in different phases (as a function of h and R_i respectively) can be minimized with respect to the h and/or R_i to yield the preferred period and hence the elastic and interfacial free energy costs of forming the ordered structure (to maintain brevity, we do not display the explicit expressions for the periods and radii in the text). A comparison of the relative free energies of the ordered phases then allows one to discern the preferred ordered phase if the system were to order. The free energy cost of the preferred ordered phase when combined with ΔF_{bulk} allows us to compare the relative preference for ordering and hence the order−disorder transition temperatures. While the formulation provides a means to rapidly determine the overall phase diagram of the system we refrain from presenting an exhaustive analysis of the influence of different parameters, and instead mainly discuss the physical insights derived from such a model and a brief comparison to the SCFT results.

B. Physical Insights From SST. Within the assumptions of our model, the main outcome of our SST calculations is the identification of the primary driving forces behind the orientational and compositional ordering. As seen from eq 28, the orientational ordering is dependent only on the parameters μ, m, and ϕ_R. The only effect of compositional ordering transitions upon the I−N transition is suggested to be a renormalization of the effective volume fraction of the rods ϕ_R which differs between the ordered (but is independent of the nature of the ordered phase) and disordered phases. Moreover, in the ordered phase ϕ_R is independent of the volume fraction of the A phase f_A. These features rationalize the fact that in the phase diagrams presented in Figures 2 and 6, where the I−N transitions occur within the ordered phases, the lines corresponding to I−N transitions (I−N) appear practically independent of f_A.

The above arguments also allow us to comment on the onset of I−N transitions relative to the order−disorder transition. Indeed, our SST model suggests that while it is certainly easier for orientational ordering to occur in the compositionally ordered phases (due to a larger effective ϕ_R), nevertheless orientational ordering in the compositionally disordered phases is also possible for appropriate parameters of μ, m, and ϕ_R^D. Moreover, since $\phi_R^D \propto 1 - f_A$, such a transition is more likely for smaller values of f_A. This conclusion is broadly consistent with the results presented in section IIIB and the experimental observations of Zheng and co-workers who had observed that for lower molecular weights and higher LC block volume fractions, the ODT coincided with the I−N transition temperature.[7]

The SST model predicts the orientational ordering to depend only on the Maier−Saupe interaction parameter μ and to be independent of the χ_1 parameter (our SCFT model fixes the ratio μ/χ_1 thereby endowing a fictitious dependence on χ_1). On the other hand, from eq 32, it is seen that the ODT can indeed be influenced by the orientational ordering if the rods are either orientationally ordered in the disordered phase itself or if the transition to the compositionally ordered phase is also accompanied by a I−N transition. In either of these instances, the orientational order parameters S_D and S_O will be such that $S_O > S_D$. From eqs 32 and 36, it can be seen that this results in a free energy preference for compositionally segregated phases, and in turn can be viewed as an increase in the effective χ_1 parameter between the A and B blocks.

Finally, for the situation when the ODT occurs between two isotropic phases, our SST model suggests that the self-assembly characteristics (including order−order transitions) expected to semiquantitatively resemble the phase behavior of conformationally asymmetric diblock copolymers. The phase diagrams presented in Figures 2 and 6 certainly accord with this expectation.

C. Comparisons of SST Results to SCFT. While the SST is much simpler to implement than SCFT calculations and provides physical insights, the model assumptions restrict its applicability to only a special class of situations. Even discounting the typical limitations of SST (i.e., its validity only for extremely strong segregations),[20] a significant assumption of our model is in our characterization that the main effect of the rod units is in its contribution to an increased monomeric volume of the B segments. This assumption is expected to be valid only under the combined situation of short rods and near perfect orientational ordering in the compositionally ordered mesophases—a combination which is extremely hard to achieve in reality. Indeed, when rods transverse more than (approximately) the segment length b of the flexible components in the XY plane (the plane of compositional ordering) they can no longer be regarded as just contributing volume to "a segment" of the backbone. Moreover, the interplay of rod orientations and the compositional inhomogeneity near the interfaces is also certain to render the expression (37) suspect for our system. On the other hand, the SCFT model suffers from no such limitations and can in principle handle arbitrarily long rods and segregations.

Considering the above aspects, it is to be expected that the comparison between SCFT and SST would at best be qualitative with the correspondences becoming better for shorter rod conditions characteristic of our SST model. Since, in our model, the rod length scales with the m parameter, this would be expected for smaller m values. In parts a−c of Figure 7, we display results which illustrate this expectation. Figure 7a presents the SST results corresponding to the SCFT results presented Figure 6 where $m = 5$ and $N = 100$. In contrast, parts b and c of Figure 7 present the SCFT and SST results

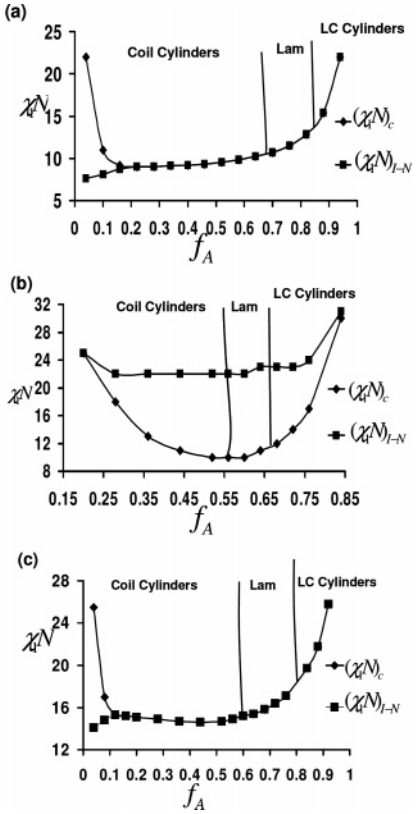

Figure 7. (a) SST phase diagram for the parameters $N = 100$ and $m = 5$. (b) SCFT phase diagram for the case $N = 100$, $m = 3$ and $\beta = 1$. (c) SST phase diagram for the case $N = 100$ and $m = 3$. In parts a and c, the I−N transition lines coincide with the ODT's for a major portion of the phase diagram.

corresponding to $N = 100$ and $m = 3$. It can be seen that while in both cases SST predicts the qualitative trends very well (including the ODT values, a regime where SST is actually expected to be inaccurate), a quantitative correspondence is achieved between the morphologies displayed in Figure 7, parts b and c, which correspond to the case of shorter rods. However, the I−N lines are observed to be shifted upward in the SCFT results compared to the SST results. This observation can be rationalized by noting that the I−N lines in SST assumed a perfect segregation of the components right at the ODT. In reality, this condition is not met until much higher $\chi_1 N$.

V. Conclusions

In this article, we have proposed a self-consistent field theoretic model and a SST based analytical theory to understand the thermodynamic behavior of side chain liquid crystalline diblock copolymers. In the SCFT model, the effect of side chain mesogenic units were accounted by incorporating rodlike units attached to every monomer of the flexible backbone. This model allowed us to combine the orientational ordering interactions of the rod segments with the mean field theory of flexible diblock copolymer. We solved the model to study the various 2D morphologies and the orientational characteristics of the rod segments as a function of molecular weight, rod length, interaction parameters, and volume fraction of each block. The morphologies observed were similar to the ones found for the case of flexible diblock copolymer, with additional possibility for smectic orientational ordering. An important result of our simulation was that for the parameter space probed, the microphase separation was a necessary condition for the development of orientational ordering. Cylindrical morphologies with the LC block in the dispersed or the continuous phases were observed. The orientational ordering was always observed to be parallel to the block copolymer interface, and in the case of cylinders, parallel to the axis of cylinders. The orientational ordering transition was observed to be favored by reducing the molecular weight of the polymer and/or by increasing the rod length. Another interesting result was the effect of orientational interactions in influencing the ODT of the block copolymer in the regime of higher volume fractions of the LC block. While we presented limited representative parametric results, the advantage of the SCFT model is that it makes the exploration of the vast parametric space involved in the system easily amenable. Moreover, extensions to SCLC with a longer alkyl spacer (modeled as another polymer),[7] multiblock SCLC, solutions of SCLC etc. can be accomplished in a straightforward manner.

The SST model was based on a simpler representation of the SCLC block copolymer as a conformationally asymmetric block copolymer. The rod units were assumed to mainly influence the effective volumes of the individual monomers except in the situation wherein the orientational ordering occurred on or before the ODT. We adapted the classical SST ideas for flexible diblock copolymers to discern the qualitative features of the phase diagram. The main utility of the SST model was in its ability to provide physical insights and thereby rationalize the observations accompanying our SCFT model. We also clarified the parametric conditions under which the SST model is expected to accord with the SCFT results and provided evidence supporting our claims. This semiquantitative comparisons obtained between SCFT and SST model does suggest that the ordering in a wider class of SCLC block copolymers may fruitfully be understood by combining many of the earlier developments in the context of flexible block copolymers with that of orientational ordering in liquid crystals.

Acknowledgment. This work was partially supported by National Science Foundation under Award CTS-0347381 and by a grant from the Robert A. Welch Foundation.

References and Notes

(1) Matsen, M. W. *J. Phys.: Condens. Matter* **2002**, *14*, R21−R47.
(2) Kato, T.; Mizoshita, N.; Kishimoto, k. *Angew. Chem., Int. Ed.* **2006**, *45*, 38−68.
(3) Pryamitsyn, V.; Ganesan, V. *J. Chem. Phys.* **2004**, *120*, 5824−5838.
(4) Chen, J. T.; Thomas, E. L.; Ober, C. K.; Mao, G. P. *Science* **1996**, *273*, 343−346.
(5) Mao, G.; Ober, C. K. *Acta Polym.* **1997**, *48*, 405−422.
(6) Roukolainen, J.; Makinen, R.; Torkelli, M.; Makela, T.; Serimaa, R.; ten Brinke, G.; Ikkala, O. *Science* **1998**, *280*, 557−560.
(7) Zheng, W. Y.; Hammond, P. T. *Macromolecules* **1998**, *31*, 711−721.
(8) Fischer, H.; Poser, S. *Acta Polym.* **1996**, *47*, 413−428.
(9) Mao, G.; Wang, J.; Clingman, S. R.; Ober, C. K.; Chen, J. T.; Thomas, E. L. *Macromolecules* **1997**, *30*, 2556−2567.
(10) Hamley, I. W.; Castelleto, V.; Lu, Z. B.; Imrie, C. T.; Itoh, T.; Al-Hussein, M. *Macromolecules* **2004**, *37*, 4798−4807.
(11) Thomas, E. L.; Chen, J. T.; O'Rourke, M. J. E.; Ober, C. K.; Mao, G. *Macromolecular Symoposia* **1997**, *117*, 241−256.
(12) Anthamatten, M.; Hammond, P. T. *Macromolecules* **1999**, *32*, 8066−8076.
(13) Osuji, C. S.; Chen, J. T.; Mao, G.; Ober, C. K.; Thomas, E. L. *Polymer* **2000**, *41*, 8897−8907.
(14) Verploegen, E.; McAfee, L. C.; Tian, L.; Verploegen, D.; Hammond, P. T. *Macromolecules* **2007**, *40*, 777−780.
(15) Anthamatten, M.; Zheng, W. Y.; Hammond, P. T. *Macromolecules* **1999**, *32*, 4838−4848.
(16) Anthamatten, M.; Hammond, P. T. *J. Polym. Sci., Part B: Polym. Phys.* **2001**, *39*, 2671−2691.
(17) Wang, R.; Jiang, Z.; Hu, J. *Polymer* **2005**, *46*, 6201−6207.
(18) Shinozaki, A.; Jasnow, D.; Balazs, A. *Macromolecules* **1994**, *27*, 2496−2502.
(19) Nap, R. J.; ten Brinke, G. *Macromolecules* **2002**, *35*, 952−959.

(20) Matsen, M. W.; Bates, F. S. *Macromolecules* **1996**, *29*, 1091−1098.
(21) Semenov, A. N. *Sov. Phys. JETP* **1985**, *61*, 733.
(22) Semenov, A. N. *Zh. Eksp. Teor. Fiz.* **1985**, *81*, 1242.
(23) Matsen, M. W.; Barrett, C. *J. Chem. Phys.* **1998**, *109*, 4108−4118.
(24) Fredrickson, G. H.; Ganesan, V.; Drolet, F. *Macromolecules* **2002**, *35*, 16−39.
(25) Matsen, M. W.; Schick, M. *Phys. Rev. Lett.* **1994**, *72*, 2660−2663.
(26) Fredrickson, G. H. *The Equilibrium Theory of Inhomogeneous Polymers*, 1st ed.; Oxford University Press: Oxford, U.K., 2006.
(27) Press, W. H. *Numerical Recipes in Fortran*, 2nd ed.; Cambridge University Press: New York, 1986.
(28) Olsen, B. D.; Segalman, R. A. *Macromolecules* **2005**, *38*, 10127−10137.
(29) Helfand, E.; Sapse, A. M. *J. Chem. Phys.* **1975**, *62*, 1327−1331.
(30) de Gennes, P. *The Physics of Liquid Crystals*; Oxford University Press: New York, 1974.

MA071566B